

## Anomalous-X-Ray-Transmission Investigation of Neutron-Irradiated Copper: Comparison of Theory and Experiment\*

B. C. Larson and F. W. Young, Jr.

*Solid State Division, Oak Ridge National Laboratory, Oak Ridge, Tennessee 37830*

(Received 29 March 1971)

In this study we have made anomalous-x-ray-transmission measurements on nearly perfect copper crystals that had been irradiated with fast neutron doses varying from 3.6 to  $10.9 \times 10^{18}/\text{cm}^2$  ( $E > 0.6$  MeV). The observed decrease in intensities for 111, 220, and 222 reflections with  $\text{Cu}K\alpha$ ,  $\text{Mo}K\alpha$ , and  $\text{Ag}K\alpha$  x rays was expressed in terms of effective absorption coefficients. These absorption coefficients increased linearly with neutron dose. They have been analyzed in terms of the theory of Dederichs, and it has been shown that these data are consistent with the presence of defect aggregates in the form of dislocation loops. It has also been shown that the theory can explain the wavelength and reflection dependence of the observed absorption coefficients for these neutron doses when the calculations are scaled to the measured data for the 111 reflections of  $\text{Mo}K\alpha$  and  $\text{Cu}K\alpha$  radiations. Therefore, these data have provided a successful test of the functional dependence of the theory, independent of the defect concentration and size distribution.

### I. INTRODUCTION

Anomalous x-ray transmission has been shown to be sensitive to small concentrations of defects in crystals, especially when the defects have aggregated into clusters or small dislocation loops; for example, oxygen precipitated in silicon,<sup>1</sup> arsenic in germanium,<sup>2</sup> and neutron-irradiation damage in silicon, germanium,<sup>3</sup> and copper.<sup>4</sup> A theoretical treatment has been given by Dederichs.<sup>5</sup> Young, Baldwin, and Dederichs<sup>6</sup> found that there was a good correlation between the decrease in anomalous-x-ray transmission and defect concentrations determined by electron microscopy for copper crystals irradiated with fast neutron doses in the range of  $10^{18}/\text{cm}^2$  ( $E > 0.6$  MeV). However, for neutron doses of the order  $10^{19}/\text{cm}^2$ , where the defect densities become large enough that overlap of defect-strain fields may be a problem, the x-ray measurements indicated a rather larger effect than that predicted from the electron-microscopy work.

In this study, additional anomalous-x-ray-transmission measurements have been made on nearly perfect copper crystals irradiated with 3.6–10.9  $\times 10^{18}$   $n/\text{cm}^2$  with the sample temperature 43 °C. These measurements have been made with three different wavelengths, and a detailed comparison of the theory with the experimental results is presented.

### II. EXPERIMENTAL PROCEDURE

The copper crystals used in this experiment were lamellae oriented such that they had (111) faces and dimensions of approximately  $1 \times 1 \times t_0$  cm,  $0.024 < t_0 < 0.092$ . The dislocation densities of these crystals were  $\sim 10^2/\text{cm}^2$ , and they were

shown to be essentially perfect from the standpoint of x-ray diffraction by Borrmann topography and integrated Borrmann intensities. The irradiations were carried out in the CP-15 facility of the bulk shielding reactor (BSR) at Oak Ridge National Laboratory. This facility utilizes a circulating helium atmosphere that is in thermal contact with the reactor-pool water to provide convection cooling of the sample during irradiation. The samples were irradiated in a reactor-spectrum flux of  $6 \times 10^{12}$   $n/\text{cm}^2/\text{sec}$  at a temperature of 43 °C as measured directly by a thermocouple attached to a dummy sample included in the irradiation capsule. Three different total doses were obtained: 3.6, 7.2, and  $10.9 \times 10^{18}$   $n/\text{cm}^2$  ( $E > 0.6$  MeV).

After irradiation the crystals were etched lightly with nitric acid to remove surface corrosion that developed during the irradiation and were attached to wire supports with salol. This mounting technique introduced no strain observable by topography or integrated-intensity measurements, and left the entire face of the sample free for measurements. The integrated-anomalous-transmission measurements were made on a double-crystal diffractometer using  $\text{Cu}K\alpha$ ,  $\text{Mo}K\alpha$ , and  $\text{Ag}K\alpha$  radiations for 111, 220, and 222 reflections.  $hkl$  and  $\bar{h}\bar{k}\bar{l}$  reflections were measured for both the diffracted and transmitted Borrmann beams in order that any strains or inconsistencies in the measurements might be detected.<sup>4,7</sup>

### III. THEORY

The integrated intensity for the diffracted beam in anomalous transmission through a perfect non-vibrating lattice is given theoretically by<sup>8,9</sup>

$$R_H = \frac{P(e^2/mc^2)\lambda^2 F'_H}{\sin(2\theta_B)V_c |b|^{1/2}} \left(\frac{1}{8\pi h}\right)^{1/2} e^{-(\mu_0 t - h)} \\ \times \left[1 + \frac{1}{8h} + \frac{9}{2}\left(\frac{1}{8h}\right)^2 + \dots\right], \quad (1)$$

where  $\lambda$  is the x-ray wavelength,  $H = 2\pi/d_{hkl}$  is the magnitude of the reciprocal-lattice vector,  $V_c$  is the volume of a primitive cell,  $e^2/mc^2$  is the classical electron radius,  $F'_H$  is the real part of the structure factor,  $\theta_B$  is the Bragg angle, and  $\mu_0$  is the linear absorption coefficient.  $b$  is given by  $\gamma_0/\gamma_H$  where  $\gamma_0$  and  $\gamma_H$  are the direction cosines of the incident and diffracted beams with the surface normal, respectively.  $t = \frac{1}{2}t_0(1/\gamma_0 + 1/\gamma_H)$  is the effective thickness of the crystal of actual thickness  $t_0$ , and  $h \approx \mu_0 t P \epsilon_0$  where  $\epsilon_0 = F''_H/F'_0$  is the ratio of the imaginary part of the structure factor for the Bragg diffracted and forward directions, respectively.  $P$  is the polarization factor and is given by 1 or  $\cos 2\theta_B$ , depending on whether the polarization of the x ray is perpendicular or parallel to the plane of diffraction.

This expression is strictly applicable only for a nonvibrating lattice so that for room-temperature measurements the effect of thermal vibrations must be considered. The well-known<sup>10-12</sup> result of including thermal vibrations is that  $\epsilon_0$  must be replaced by  $\epsilon_0 e^{-M_H}$ , and  $F'_H$  must be replaced by  $F'_H e^{-M_H}$ , where  $M_H$  is the thermal Debye-Waller factor. In addition to this effect, thermal vibrations give rise to diffusely scattered x rays (thermal diffuse scattering) that are no longer anomalously transmitted and are therefore absorbed by the photoelectric process. Thus diffuse scattering reduces the transmitted intensity and must in principle be considered. However, theoretical and experimental determinations<sup>13,14</sup> of this effect indicate that it amounts to at most a few percent at room temperature and can in practice be neglected in most cases.

When point defects or clusters of point defects are present in the lattice, there are, in addition to the dynamical-thermal displacements of the atoms, static displacements of those atoms lying in the strained region surrounding the defects. Dederichs<sup>5,15</sup> has recently treated the effect of point defects and of aggregations of defects into clusters or loops on the anomalous transmission. Such aggregates have been observed after room-temperature neutron irradiations and impurity-precipitation experiments. The theory shows a very large increase in the absorption of the anomalously transmitted x-ray beam for clustered defects compared to that expected for the same number of point defects randomly distributed. This result is in agreement with the experimental measurements, so we consider now only the case of

clustered defects.

It is possible to understand the general nature of the effects on anomalous transmission of such defect clusters by analogy with thermal-vibrational effects. As shown by Dederichs,<sup>5</sup> for clustered defects it is the displacements of the atoms surrounding the defect regions and not the defect atoms themselves that are predominantly responsible for the decrease in anomalous transmission. Hence, clustered defects may be expected to produce an additional contribution to the Debye-Waller factor as a result of their static displacements, and also an additional amount of diffuse scattering arising from the correlations of static displacements. These are in fact the essential components in the theory of Dederichs and so the intensity transmitted through a crystal containing defect clusters can be written

$$R_H = \frac{P(e^2/mc^2)\lambda^2 F'_H e^{-(M_H + L_H)}}{\sin(2\theta_B)V_c |b|^{1/2}} \left(\frac{1}{8\pi h}\right)^{1/2} \\ \times \exp[-\mu_0 t(1 - P\epsilon_0 e^{-(M_H + L_H)})] \\ \times \left(1 + \frac{1}{8h} + \dots\right) e^{-\mu_{DS} t}. \quad (2)$$

The thermal Debye-Waller factor  $M_H$  has been replaced by  $M_H + L_H$ , and the effect of defect diffuse scattering has been represented by an absorption coefficient  $\mu_{DS}$ .  $L_H$  is the Debye-Waller factor associated with static displacements and is given by  $H^2 \langle s^2 \rangle / 6$  where  $\langle s^2 \rangle$  is the mean-square atomic displacement resulting from the defects. When the defects are aggregated loosely (without relaxation) into regions of radii  $R_{c1}$  the static Debye-Waller factor is given by

$$L_H \approx \frac{H^2}{6} c \left(\frac{4\pi A^2}{V_c}\right) \frac{n_{c1}}{R_{c1}}, \quad (3)$$

where  $c$  is the concentration of point defects in the lattice (i. e., the number of defects/number of lattice sites).  $n_{c1}$  is the number of point defects in the cluster, and  $A$  is related to the volume change  $\Delta V$  of the crystal resulting from the production of a point defect by  $\Delta V = 4\pi A^3(1 - \nu)/(1 + \nu)$ .  $\nu$  is the Poisson ratio. If the aggregate becomes dense enough that there is significant relaxation due to the interaction of the point defects so that they collapse into dislocation loops, the Debye-Waller factor is then given by

$$L_H = \frac{c R_0 b^{1/2} H^{3/2}}{2\pi} = \frac{C_L R_0^3 (Hb)^{3/2}}{2V_c}. \quad (4)$$

$C_L = c/n_L$  is the concentration of loops with  $n_L = b\pi R_0^2/V_c$  point defects per loop,  $R_0$  is a radius defined such that the area of the not necessarily circular loop is given by  $\pi R_0^2$ , and  $b$  [not to be con-

fused with  $b$  in Eq. (1)] is here the magnitude of the Burgers vector of the loop.

In Eq. (2),  $L_H$  enters essentially as  $e^{-L_H/2}$  in the prefactor and as  $\exp[-\mu_0 t P \epsilon_0 e^{-M_H} (1 - e^{-L_H})]$  in the exponential

$$\begin{aligned} \mu_0 t (1 - P \epsilon_0 e^{-(M_H + L_H)}) &= \mu_0 t (1 - P \epsilon_0 e^{-M_H}) \\ &+ \mu_0 t P \epsilon_0 e^{-M_H} (1 - e^{-L_H}). \end{aligned}$$

For typical  $\mu_0 t$  values of 10–40, only the latter term is significant and a photoelectric absorption coefficient

$$\mu_{PE} = \mu_0 P \epsilon_0 e^{-M_H} (1 - e^{-L_H}) \quad (5)$$

can be defined. For  $L \ll 1$ ,  $\mu_{PE} \approx \mu_0 P \epsilon_0 e^{-M_H} L_H$ .

The absorption coefficients for the diffuse-scattering contributions due to aggregates of defects are given by

$$\mu_{DS} = cJ(\lambda, H) n_{cl} \ln \left( \frac{D}{R_{cl}} \right) \left( \frac{4\pi A \cos \theta_B}{V_c} \right)^2 \quad (6)$$

for clusters, and the expression for loops is

$$\begin{aligned} \mu_{DS} &= cJ(\lambda, H) n_L \ln \left( \frac{D}{R_0} \right) \\ &\times \left[ \frac{8}{15} + \frac{1}{15} \left( \frac{2\nu^2 + 6\nu - 1}{(1 - \nu)^2} \right) \cos^2 \theta_B \right], \quad (7) \end{aligned}$$

where  $k = 2\pi/\lambda$ ,  $D$  is the extinction length for the reflection excited and

$$J(\lambda, H) = \frac{\pi}{V_c} \left( \frac{H}{k} \frac{e^2}{mc^2} P F'_H e^{-(M_H + L_H)} \right)^2. \quad (8)$$

This absorption coefficient is now additive with  $\mu_{PE}$  to obtain an effective absorption coefficient  $\mu^* = \mu_{PE} + \mu_{DS}$ . With reference to Eq. (1) the observed intensity transmitted through the defect crystal is given by

$$R_H(\text{obs}) = R_H(\text{calc}) e^{-\mu^* t}, \quad (9)$$

where thermal vibrations have been included in  $R_H(\text{calc})$ .

Comparing the expressions for the photoelectric absorption and diffuse-scattering absorption we can see that  $\mu_{PE}$  depends mainly on  $\mu_0$  and  $L_H$ , which

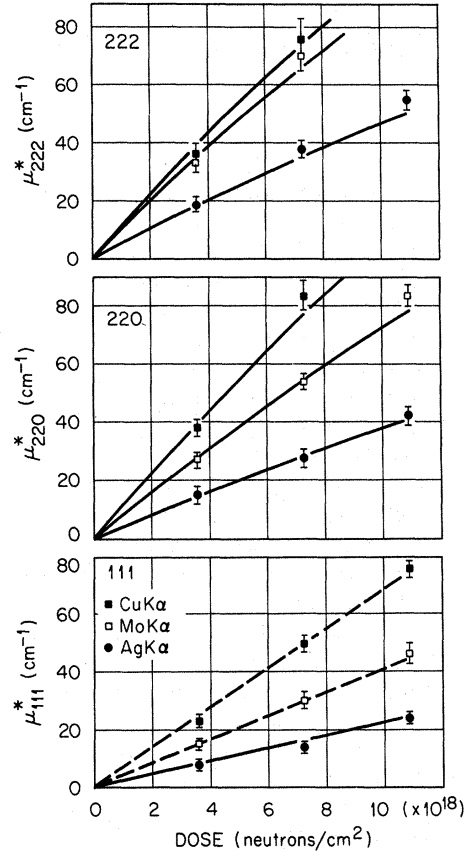


FIG. 1. Effective absorption coefficients vs neutron dose. The solid lines were calculated from the dashed lines. The points are the data from Table I.

is proportional to either  $H^2$  or  $H^{3/2}$ , depending on whether clusters or loops are predominant. In contrast to this  $\mu_{DS}$  depends on  $F'_H{}^2 H^2 \lambda^2$  for both clusters and loops. As pointed out by Dederichs,<sup>5</sup> the diffuse scattering is determined by the asymptotic displacement fields of the aggregates which are both proportional to  $r^{-2}$ , resulting in the same functional dependences, while the Debye-Waller factor contains more effects relating to displacements near the core of the defect aggregates which are different for the two cases, resulting in the different  $H$  dependences.

TABLE I. Effective absorption coefficients of  $\mu^*$ . For  $R_H(\text{calc})$ ,  $\theta_D = 306^\circ$  was used, and other constants from Baldwin, Young, and Merlini (Ref. 16).

Dose ( $n/\text{cm}^2$ ) wavelength	$3.6 \times 10^{18}$			$7.2 \times 10^{18}$			$10.9 \times 10^{18}$		
	Cu K $\alpha$	Mo K $\alpha$	Ag K $\alpha$	Cu K $\alpha$	Mo K $\alpha$	Ag K $\alpha$	Cu K $\alpha$	Mo K $\alpha$	Ag K $\alpha$
$\mu_{111}^*$ ( $\text{cm}^{-1}$ )	23	15	8	49	30	14	75	46	24
$\mu_{220}^*$ ( $\text{cm}^{-1}$ )	38	27	15	84	54	28	...	84	43
$\mu_{222}^*$ ( $\text{cm}^{-1}$ )	36	34	19	76	70	37	...	...	54

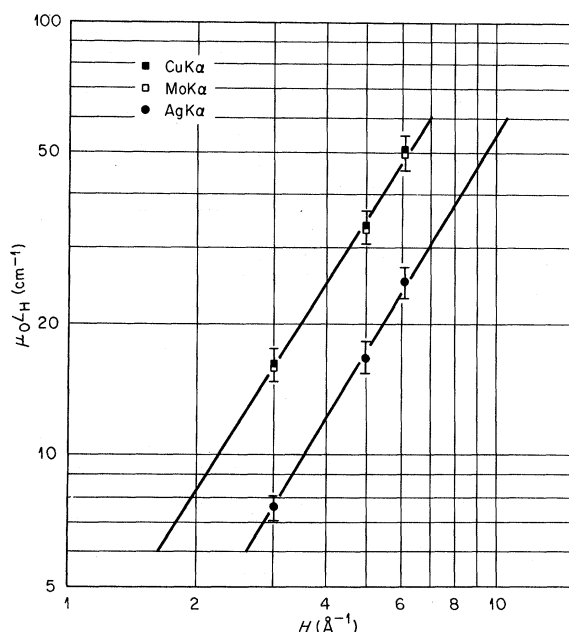


FIG. 2.  $H$  dependence of the static Debye-Waller factor. These  $L$  values range from 0.036 to 0.112.

#### IV. RESULTS

Equation (9) has been used to calculate the absorption coefficients from the integrated intensity measurements made on the irradiated samples. These data are given in Table I and represent the averages of several measurements of both the forward transmitted and diffracted intensities for  $hkl$  and  $\bar{h}\bar{k}\bar{l}$  reflections on two crystals for the lower and intermediate doses and on one crystal for the higher dose. They are shown graphically in Fig. 1, where the effective absorption coefficients are plotted as a function of neutron dose for the three wavelengths and the reflections measured.

From the plots of the absorption coefficients vs dose there appears to be a linear increase in the damage with increasing dose. Since there is a distribution in the size of the aggregates produced by neutron irradiation,<sup>17,18</sup> the linear increase indicates a linear increase of the product of concentration of defect clusters (loops) and the appropriate moment of the radius. A linear increase was observed previously<sup>6</sup> using another reactor for the same neutron dose. In the present study the slope is  $\sim 5\%$  greater for  $\text{CuK}\alpha$ , which may be within the errors of the two sets of measurements. However, the greater slope may indicate a small difference in the defect size distributions.

Qualitatively the wavelength and reflection dependence of the coefficients are in agreement with the theory, which predicts a larger absorption for the longer wavelengths and also an increase in

absorption for the higher-order reflections. Since the theory predicts  $\mu_{\text{PE}}$  for  $\text{CuK}\alpha$  and  $\text{MoK}\alpha$  to be nearly equal and the diffuse-scattering absorption (being proportional to  $\lambda^2$ ) to be almost five times larger for  $\text{CuK}\alpha$ , the observed difference between  $\mu^*$  for these two wavelengths is an indication of the size of the  $\text{CuK}\alpha$  diffuse-scattering component. For the 111 reflection and  $\text{CuK}\alpha$  radiation it is apparent that  $\mu_{\text{DS}}$  is comparable to  $\mu_{\text{PE}}$ , which is in marked contrast to the small effects produced by diffuse scattering from thermal displacements.

In order to obtain information about the damage structure from these measurements, it is necessary to consider them in terms of the detailed predictions of the theory. The theory as outlined above contains a number of predictions as to the wavelength, order, and dose dependences of the absorption coefficients that can be used to extract information as to the size, configuration, and concentration of the defect regions. This has been demonstrated with the previous measurements<sup>6</sup>; however, the present measurements are somewhat more complete and offer the possibility of a more detailed examination of the theory.

The defect configurations considered by the theory are those of point defects loosely aggregated into spherical clusters and of defects more densely aggregated into planar dislocation loops. According to Eqs. (3) and (4) the  $H$  dependence of the static Debye-Waller factor  $L_H$  can be used to distinguish between these two configurations. The  $H$  and  $\lambda$  dependences of the diffuse-scattering absorption are the same for both configurations and it is therefore possible to separate the measured absorption coefficients into photoelectric and diffuse-scattering components without making any assumptions as to the  $H$  dependence of  $L_H$ . Assuming the theoretical forms of the coefficients and choosing the values for a dose of  $5 \times 10^{18}$  from a linear fit to all the data, we have made these separations by solving simultaneous equations that satisfy the data for pairs of wavelengths.

The values of  $L_H$ , which were obtained from these values of  $\mu_{\text{PE}}$  through Eq. (5), are plotted as  $\mu_0 L_H$  against  $H$  in Fig. 2. (This method of plotting serves to separate the data for the different wavelengths.) The assumption  $\bar{h} \approx \mu_0 t P \epsilon_0 e^{-MH}$  used in deriving Eq. (5) is no longer valid for the asymmetric 222 reflection of  $\text{CuK}\alpha$ , and the exact expression was used to calculate the plotted value for this reflection. The slopes of these plots are about 1.6, i. e., nearly  $\frac{3}{2}$  which indicates the predominant defect configuration to be dislocation loops, in agreement with electron microscopy studies of fast neutron-irradiated copper.<sup>17,18</sup>

From the individual components of the absorption coefficients it is possible to obtain information about the product of the defect concentration

and the radii. [These are related to the third and fourth moments of the defect radii as defined in Eqs. (4) and (7).] In order to get unambiguous information from these products, it is necessary to have an independent measurements of one of them; however, it is possible to use  $\mu_{PE}$  and  $\mu_{DS}$  values calculated from the data for the 111 reflection of  $CuK\alpha$  and  $MoK\alpha$ , as averaged by the dashed lines in Fig. 1, and Eqs. (5) and (7) to compute  $\mu^*$  values for the other reflections and wavelength. This makes it possible to compare the  $\lambda$  and  $H$  dependences of the theory with the measured data without the use of the concentration and size distributions of the defects. These calculated values are represented by the solid lines in Fig. 1 and can be seen to be in satisfactory agreement with the remainder of the observed data points. This is especially true for the  $AgK\alpha$  radiation, since no data for this wavelength were used in the scaling procedure. It is interesting to note that even though

these lines were generated from straight lines through the 111 data, the lines from the higher-order calculations are somewhat curved in the higher-dose range. This is a result of the fact that for the higher-order reflections the value of  $L_H$  becomes large enough that the factor  $(1 - e^{-L_H})$  begins to deviate from  $L_H$ , and the diffuse-scattering absorption is more significantly affected by the factor  $e^{-2L_H}$ . There does not seem to be any noticeable curvature in the measured data as a function of dose; however, a slight increase in the average size of the defect regions as a function of dose would produce a curvature of the opposite sense and tend to cancel the predicted curvature. This effect is in any case barely outside the experimental error and may be obscured. We conclude from this satisfactory agreement between the observed and calculated values that the functional dependencies of the theory are adequate to account for the data.

\*Research sponsored by the U.S. Atomic Energy Commission under contract with Union Carbide Corp.

<sup>1</sup>J. R. Patel and B. W. Batterman, *J. Appl. Phys.* **34**, 2716 (1963).

<sup>2</sup>O. N. Efimov, E. G. Sheikhet, and L. I. Datsenko, *Phys. Status Solidi* **38**, 489 (1970).

<sup>3</sup>T. O. Baldwin and J. E. Thomas, *J. Appl. Phys.* **39**, 4391 (1968).

<sup>4</sup>T. O. Baldwin, F. A. Sherrill, and F. W. Young, Jr., *J. Appl. Phys.* **39**, 1541 (1968).

<sup>5</sup>P. H. Dederichs, *Phys. Rev. B* **1**, 1306 (1970).

<sup>6</sup>F. W. Young, Jr., T. O. Baldwin, and P. H. Dederichs, in *Vacancies and Interstitials in Metals*, edited by A. Seeger, D. Schumacher, W. Schilling, and J. Diehl (North-Holland, Amsterdam, 1970).

<sup>7</sup>B. Okkerse and P. Penning, *Phillips Res. Rept.* **18**, 82 (1963). In the present work differences in the  $hkl$  and  $\bar{h}\bar{k}\bar{l}$  intensities were usually less than 5%. However, one crystal had differences as much as 10%.

<sup>8</sup>Norio Kato, *J. Phys. Soc. Japan* **10**, 46 (1955).

<sup>9</sup>R. M. Nicklow, F. A. Sherrill, and F. W. Young, Jr., *Phys. Rev.* **137**, 1417 (1965).

<sup>10</sup>P. H. Dederichs, *Physik Kondensierten Materie* **5**, 347 (1966).

<sup>11</sup>A. M. Afanasev and Yu. Kagan, *Acta Cryst.* **A24**, 163 (1967).

<sup>12</sup>Y. H. Ohtsuki, *J. Phys. Soc. Japan* **21**, 2300 (1966).

<sup>13</sup>O. N. Efimov, *Phys. Status Solidi* **22**, 297 (1967).

<sup>14</sup>H. Sano, K. Ohtaka, and Y. H. Ohtsuki, *J. Phys. Soc. Japan* **27**, 1254 (1969).

<sup>15</sup>P. H. Dederichs, *Phys. Status Solidi* **23**, 377 (1967).

<sup>16</sup>T. O. Baldwin, F. W. Young, Jr., and A. Merlini, *Phys. Rev.* **163**, 591 (1967).

<sup>17</sup>M. Rühle and J. C. Crump, *Phys. Status Solidi* **a2**, 257 (1970).

<sup>18</sup>M. Rühle, F. Häussermann, and M. Rapp, *Phys. Status Solidi* **39**, 609 (1970).